

# INTEGRAL IBIS/ISGRI energy calibration

## OSA 10

I. Caballero<sup>1</sup>, J. A. Zurita Heras<sup>2,3</sup>, F. Mattana<sup>2,3</sup>, S. Soldi<sup>1</sup>  
P. Laurent<sup>2</sup>, F. Lebrun<sup>2</sup>, L. Natalucci<sup>4</sup>, M. Fiocchi<sup>4</sup>, C. Ferrigno<sup>5</sup>, R. Rohlfs<sup>5</sup>

<sup>1</sup>AIM, CEA-Saclay, 91191 Gif sur Yvette, France

<sup>2</sup>APC (UMR 7164 Université Paris Diderot, CNRS/IN2P3, CEA/DSM,  
Observatoire de Paris), 10 rue A. Domon et L. Duquet, 75205, Paris Cedex 13, France

<sup>3</sup>François Arago Centre, APC (UMR 7164 Université Paris Diderot, CNRS/IN2P3, CEA/DSM,  
Observatoire de Paris), 13 rue Watt, F-75205 Paris Cedex 13, France

<sup>4</sup>INAF-Istituto di Astrofisica e Planetologia Spaziali, Area Ricerca CNR/Roma 2 - Tor Vergata,  
Via del Fosso del Cavaliere, 100, 00133 Rome, Italy

<sup>5</sup> ISDC Data Centre for Astrophysics, University of Geneva,  
Chemin d'Écogia 16, CH-1290, Versoix, Switzerland

June 29, 2012

## Contents

<b>1</b>	<b>Energy calibration</b>	<b>2</b>
1.1	Energy calibration with OSA 9 . . . . .	2
1.2	New energy calibration - OSA 10 . . . . .	2
1.2.1	Temperature correction . . . . .	2
1.2.2	Correction of gain and offset drifts along the mission . . . . .	3
1.2.3	Low threshold correction . . . . .	3
<b>2</b>	<b>Spectral analysis</b>	<b>3</b>

# 1 Energy calibration

## 1.1 Energy calibration with OSA 9

The ISGRI spectral gain has been observed to decrease with time. With the Offline Scientific Analysis (OSA) v9, the description of the gain drift is based on IREM counters integrated over time, to take into account the solar flares. The drift in the gain can be followed using the 511 keV line produced by the onboard radioactive  $^{22}\text{Na}$  and the fluorescence of tungsten (W) at 58.8297 keV<sup>1</sup>. However, this correction is not valid along the whole mission, as shown in Fig. 1 (black diamonds). Since IJD  $\sim 2763$  (revolution number  $\sim 583$ ), the position of the lines shows a gradual increase with time.

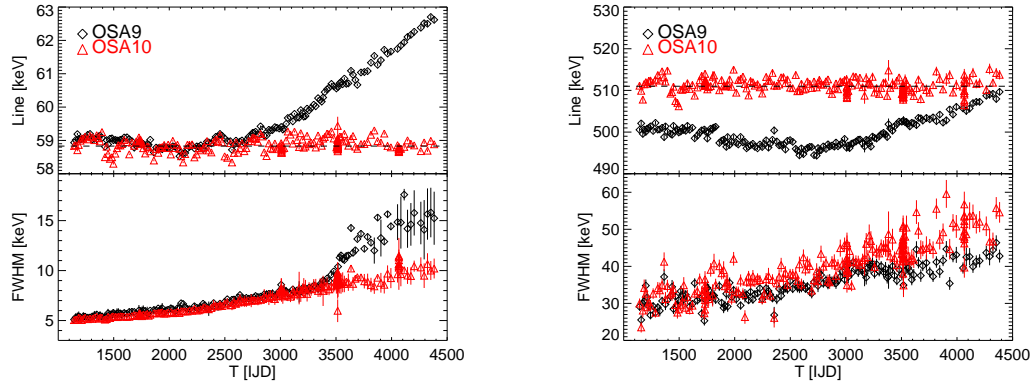


Figure 1: *Left:* Evolution of W line position (top) and FWHM (bottom) obtained with OSA 9 (black) and OSA 10 (red). *Right:* Evolution of  $^{22}\text{Na}$  line position (top) and FWHM (bottom) obtained with OSA 9 (black) and OSA 10 (red). The dashed horizontal lines in the upper panels represent the nominal positions of the W and  $^{22}\text{Na}$  lines.

## 1.2 New energy calibration - OSA 10

### 1.2.1 Temperature correction

The temperature and tension dependence of the gains and offsets of rise time and pulse height was evaluated on ground and in flight (Terrier et al. 2003, A&A, 411, L167). In OSA versions later than OSA 7, a correction of the gains-offsets depending on the ISGRI modules (MDU) temperature was performed. However, this correction assumed a constant  $\Delta T$  between the different MDUs, which is not a correct assumption along the mission. Thus, in OSA 9, the real difference in temperature between the different MDUs was not taken into account.

A more accurate temperature correction is introduced in OSA 10 using the temperatures from the ISGRI thermal probes instead of assuming a constant  $\Delta T$  along the mission between the different modules.

---

<sup>1</sup>Mean energy obtained between the  $K\alpha 1$  (59.3 keV) and  $K\alpha 2$  (57.98 keV) lines (NIST) using the ratio  $I(\alpha 2)/I(\alpha 1)=0.57$  from Kasagi et al. 1995 (Phys. Rev. A 34, 2480, 1986).

### 1.2.2 Correction of gain and offset drifts along the mission

The pulse height gain and offset in OSA 10 are described as a function of the events rise time and the time. We used data from revolutions 42–1106 to determine the gain and offset using the W and  $^{22}\text{Na}$  background lines. As shown in Fig. 1, with OSA 10, both background lines show a remarkably stable behavior with a relative energy variation below 1% around the nominal position (>6% in OSA 9). The energy resolution increases by a factor of  $\sim 2$  ( $\sim 3$  in OSA 9) between revolutions 39 and 1142.

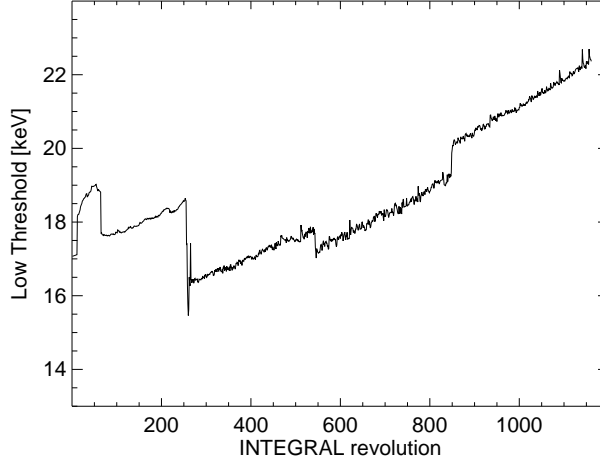


Figure 2: Low threshold position with OSA 10.

### 1.2.3 Low threshold correction

The low threshold (LT) correction has been updated in OSA 10 with the new energy correction, as shown in Fig. 2. In addition, while in OSA 9 the resolution at the low threshold energy was fixed and corresponded to that of the W line at  $\sim 59$  keV at the beginning of the mission, in OSA 10, a time dependent scaling of the resolution (as also noted for the W line) is the best solution to improve the low threshold correction (see Crab and background spectra for OSA 9 and OSA 10 in Figs. 3, 4):

$$\sigma = (FWHM_0 + FWHM_1 * revolution) / 2.36 \text{ keV} \quad (1)$$

where  $FWHM_0 = 4.80$  keV and  $FWHM_1 = 1.7 \times 10^{-3}$  keV, that replaces  $\sigma = 5.6 / 2.36$  keV in OSA 9. These values were tuned using Crab spectra at different epochs (72 revolutions spread between 39 and 1096) in order to obtain a stable spectral behavior in the  $\sim 18 - 30$  keV energy range.

## 2 Spectral analysis

The Crab and background spectra extracted with OSA 9 and OSA 10 are shown in Figs. 3 and 4. By comparing Fig. 3 (left and right), we can see that the OSA 10 correction results in less dispersion in the spectra along the mission compared to OSA 9.

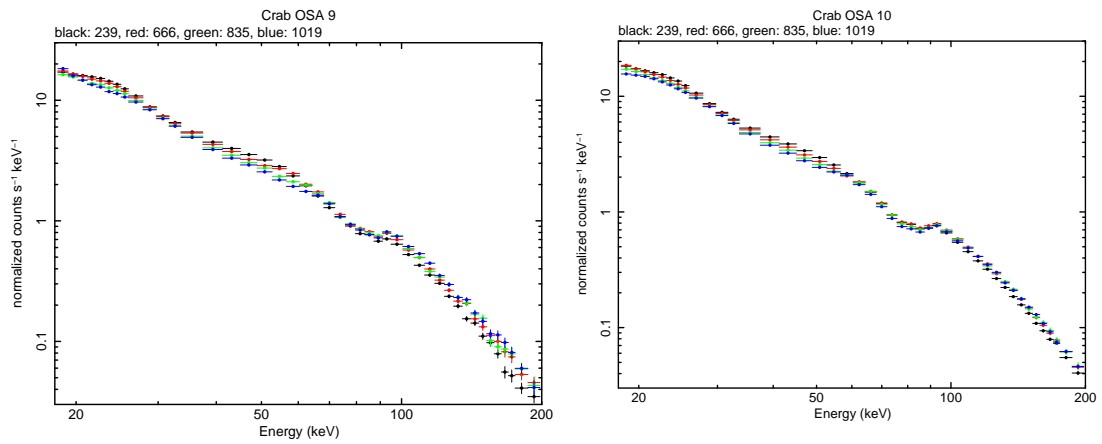


Figure 3: Crab spectra for a sample of revolutions extracted with OSA 9 (*left*) and OSA 10 (*right*).

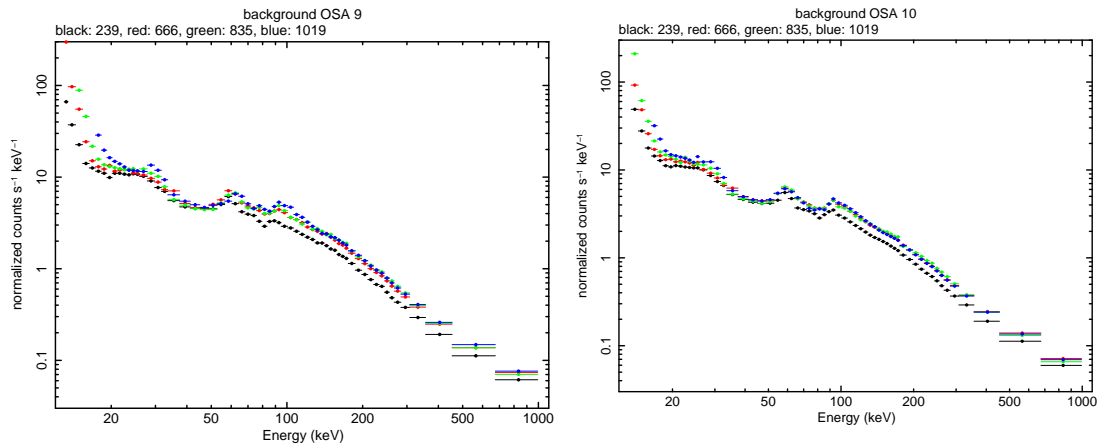


Figure 4: Background spectra for a sample of revolutions extracted with OSA 9 (*left*) and OSA 10 (*right*).

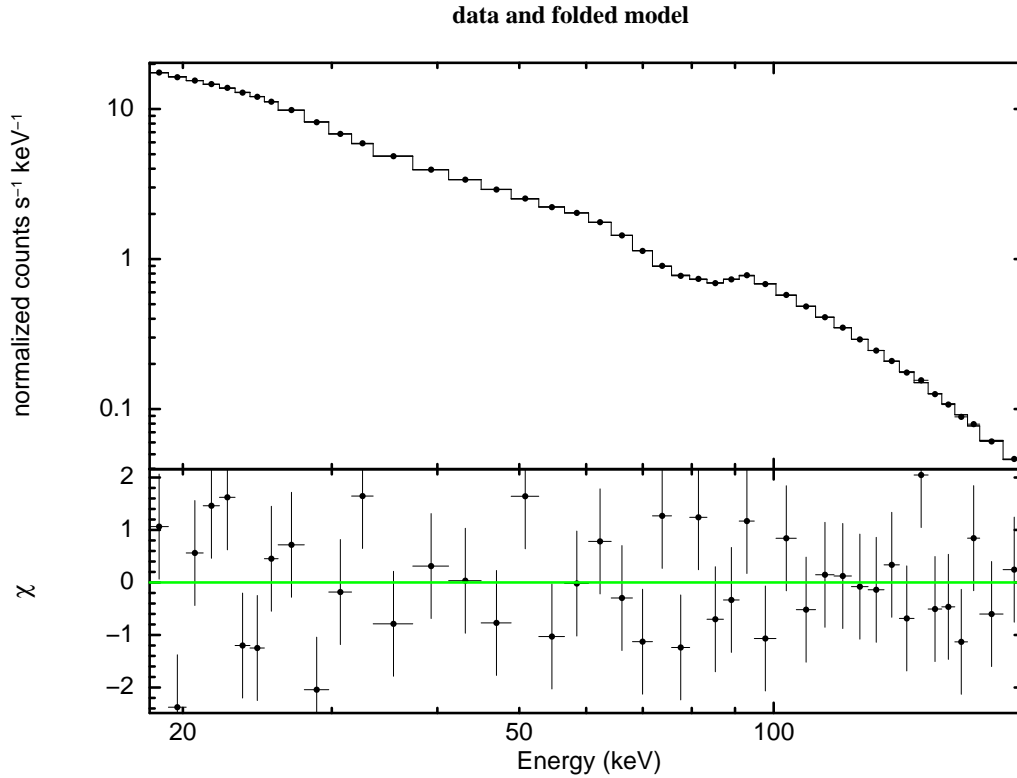


Figure 5: ISGRI Crab spectrum for revolution 839 (top) and residuals of best fit model (bottom) extracted with OSA 10.

A set of ARFs for different epochs has been produced using Crab observations. An example of a fit of the Crab spectrum from revolution 839 extracted with OSA 10 is shown in Fig. 5. The fit parameters reported in Table 1 are in good agreement with the expected values.

Table 1: Best fit parameters for the ISGRI Crab observation in revolution 839. 0.3% systematic errors were included. The quoted errors are at 90% confidence level.

$\Gamma_1$	$\Gamma_2$	$E_{\text{break}}$ [keV]	norm	$\chi_{\text{red}}^2/\text{d.o.f.}$
$2.070 \pm 0.003$	$2.24 \pm 0.03$	$94_{-5}^{+6}$	$8.6 \pm 0.1$	1.15/40

The limitations of the current energy calibration and known issues that the user should be aware of are given in the IBIS Analysis User Manual, section “Known Limitations”.